# Boundary-Element Method for Three-Dimensional Heat Transfer in Regions with Symmetry

G. E. Giles* and M. W. Wendel†
*Martin Marietta Energy Systems, Inc., Oak Ridge, Tennessee*
and
L. J. Gray‡
*Oak Ridge National Laboratory, Oak Ridge, Tennessee*

**Steady-state heat transfer through a contact region (circular and elliptical) is solved numerically by the boundary element method. With the symmetry of the problem exploited, specialized Green's functions are employed, thereby considerably simplifying the task of constructing an appropriate mesh (i.e., highly refined near the contact edge). Moreover, accurate fluxes for this difficult problem are obtained utilizing a new extrapolation technique for treating the edge discontinuity. The application of specialized Green's functions is also illustrated in another three-dimensional problem of practical importance, that of temperature profiles in an electrochemical plating cell.**

## Nomenclature

| | |
|---|---|
| $a$ | = circular contact radius |
| $G_P(X,X_0)$ | = point-source Green's function |
| $G_S(X,X_0)$ | = specialized Green's function |
| $k$ | = thermal conductivity |
| $n$ | = surface normal |
| $T$ | = temperature |
| $T_0$ | = temperature of the contact |
| $\partial D$ | = boundary surface |
| $\delta(X,X_0)$ | = Dirac delta function |
| $\psi(X_0)$ | = internal solid angle at $X_0$ |

## Introduction

THE boundary element method[1] is known to be an efficient technique for the solution of steady-state heat-transfer problems.[2-4] If we use a Green's function (fundamental solution), Laplace's equation is transformed into an integral equation on the boundary of the region; this equation is then approximated by a finite system of linear equations. An important feature of this method is the ability to tailor the Green's function to suit a specific situation (e.g., regions with symmetry). The purpose of the present paper is to demonstrate the benefits of using this technique for three-dimensional thermal problems of practical interest.

Heat transfer between contacting nonconforming surfaces has been extensively investigated, both analytically and numerically, because of its practical importance. An excellent reference to the vast literature on this subject can be found in the thesis of Currie.[5] The physical problem has been modeled by many different geometries and boundary conditions; one possibility, shown in Fig. 1, has a circular contact area at fixed temperature $T_0$, the bottom face of the cylinder at temperature $T_1$, and all other surfaces are insulated.[6,7] The singular behavior of the heat flux at the boundary edge of the contact provides a significant obstacle to an accurate numerical solution; contact regions with high eccentricity, which arise in reactor safety analyses,[8] are especially difficult.

Integral equation methods for steady-state contact problems were first investigated by Yovanovich[9] and Schneider.[3] This latter paper uses a boundary-element formulation in a half-space geometry (i.e., an exterior boundary value problem). The Unsteady Surface Element Method[10] (USE) is closely related to the boundary-element approach and has been successfully applied to transient thermal contact problems.[11] As in the USE method, an important advantage of the boundary element formulation is the inclusion of boundary conditions in the "fundamental solution" or integral kernel. By enforcing the symmetry within the Green's function, the boundary surface adjoining the contact region is eliminated from the computational model; it is therefore possible to have a highly refined discretization on the contact without the penalty of an enormous number of nodes and elements. This technique allows an accurate solution and considerably simplifies the construction of the discretization.

As might be expected, the boundary element method is not immune to problems caused by the discontinuity in the normal derivative across the contact edge: a "standard" boundary element approximation exhibits inaccurate fluxes in this area. To deal with this singularity, a new extrapolation technique has been implemented in the algorithm, greatly improving the accuracy of the solution.

Although the use of specialized Green's functions within the boundary element framework is not a new technique,[1,12] most reported applications have been for two-dimensional problems. The advantages, in terms of computational expense, mesh construction time, and accuracy of solution, for complicated three-dimensional regions are seemingly not widely appreciated.[13] To further illustrate the elegance of the boundary element approach to this class of thermal problems, an application related to electrochemical plating will be described. In a plating process, heat is generated as a consequence of the electrochemical reactions at the electrode surfaces and current flow in the cell. The electrical conductivity of the electrolyte is usually strongly dependent on the temperature; thus, the temperature distribution at the cathode can significantly impact the plating rate. Solution of the thermal problem is therefore required for an accurate modeling of the plating pro-

Received April 3, 1987; presented as Paper 87-1551 at the 22nd AIAA Thermophysics Conference, Honolulu, HI, June 8-10, 1987, revision received Oct. 22, 1987. 

*Computing Applications Consultant, Computing and Telecommunications Division. Member AIAA.
†Computing Applications Specialist, Computing and Telecommunications Divison. Member AIAA.
‡Mathematician, Engineering Physics and Mathematics Division.

cess. A realistic plating cell configuration, with the cathode in the center and four cylindrical anodes at the corners of the tank, is shown in Fig. 2. However, the thermal analysis presented in this paper is not intended to be a complete model for the electrochemical processes in the cell; it is viewed as only the first step toward a reasonable representation of the problem. The chosen boundary conditions, therefore, are an idealization of the actual state of affairs. In particular, the ohmic heating in the electrolyte is ignored and, rather than being a function of the current density, the heat flux on the electrodes is assumed constant. Nevertheless, this model serves to demonstrate the usefulness of the technique, and it is expected that a more realistic statement of the physical problem can be attacked in a similar fashion.

## Boundary Elements

The starting point of the boundary element analysis of Laplace's equation, $\nabla^2 T=0$, is the equivalent integral equation

$$\Psi(X_0)T(X_0)+\oint_{\partial D} T(X)\nabla G(X,X_0)\cdot n\,dS = \oint_{\partial D} G(X,X_0)\nabla T(X)\cdot n\,dS \tag{1}$$

The surface integral (with respect to $X$) is over the boundary of the region $\partial D$, $\Psi(X_0)$ is the internal solid angle divided by $4\pi$ at the boundary point $X_0$, and $G(X,X_0)$ is the Green's function. The function $G(X,X_0)$ is a fundamental solution of Laplace's equation, provided

$$\nabla^2 G(X,X_0) = -\tfrac{1}{2}\delta(X,X_0) \tag{2}$$

where $\delta(X,X_0)$ is the Dirac delta function.

The most common choice for $G$ is the point-source potential

$$G_P(X,X_0)=\frac{1}{4\pi\|X-X_0\|} \tag{3}$$

where $\|X-X_0\|$ is the distance between $X$ and $X_0$. This choice, however, is not the only possibility. If, for example, the three coordinate planes $x=0$, $y=0$, $z=0$ are symmetry planes, then there is no flux through these surfaces. A point source at a surface node $X_0=(x_0,y_0,z_0)$, combined with sources at the seven points obtained by reflecting through these planes, generates a Green's function

$$G_S(X,X_0)=\sum_{j=0}^{7} G_P(X,X_j) \tag{4}$$

where $X_j=(\pm x_0,\pm y_0,\pm z_0)$, which satisfies the prescribed boundary conditions on the coordinate planes. Since the Green's function $G_S$ incorporates the correct boundary values, it is not necessary to include these surfaces in the calculation. This Green's function will be employed for the solution of the contact and plating problems.

The numerical solution of Eq. (1) proceeds by decomposing the remaining pieces of the boundary $\partial D$ into elements for our purposes, triangles. The $N$ vertices of the elements are called nodes. The temperature and flux on each element are approximated by linear interpolation of the nodal values. For a particular choice of $X_0$, the integrals in Eq. (1) can be evaluated, yielding a linear expression in the $2N$ temperature and flux values at the nodes. Writing Eq. (1) for each node therefore produces a system of $N$ linear equations. As the boundary conditions supply either $T(X_0)$ *or* $\nabla T(X_0)\cdot n$, these equations are sufficient to determine the unknown quantities. If we know all of the information on the boundary, any interior temperature, if needed, can be found by applying Eq. (1).

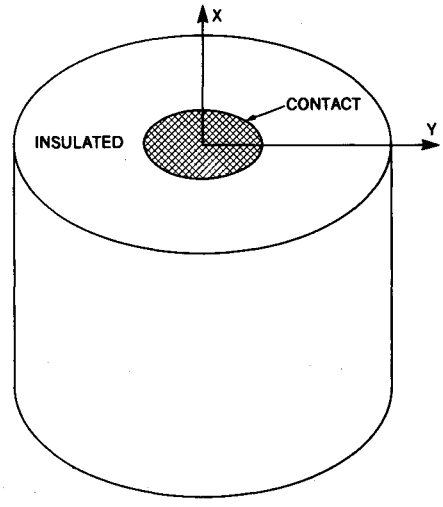


**Fig. 1 Circular contact conceptual model.**

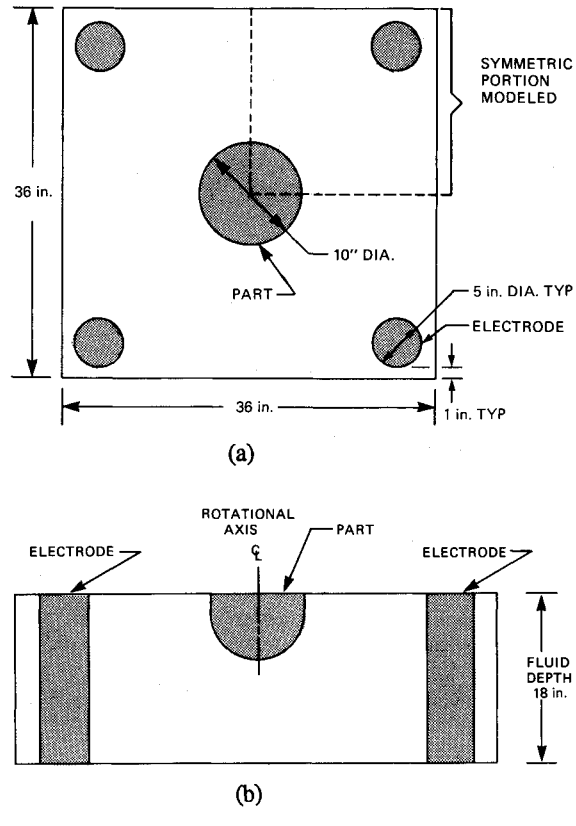


**Fig. 2 Electroplating tank: a) top view and b) section along the diagonal.**

## Contact Problem

### Circular Contact

A circular contact area in a half-space with a specified constant temperature has an exact analytic solution[14] and therefore serves as an excellent test of the computational method. If we denote the contact temperature by $T_0$, the solution is given by

$$T=\frac{2T_0}{\pi}\int_0^\infty e^{-\lambda|z|}J_0(\lambda r)\sin(\lambda a)\frac{d\lambda}{\lambda} \tag{5}$$

where $a$ is the radius of the spot and $r=(x^2+y^2)^{1/2}$. If we differentiate Eq. (5) with respect to $z$ and evaluate at $z=0$, the

flux on the contact, $0 \le r < a$, is

$$-k\frac{\partial T}{\partial z}\bigg|_{z=0} = \frac{2kT_0}{\pi(a^2 - r^2)^{1/2}} \tag{6}$$

Note that the flux becomes infinite as $r \to a^-$ and is zero for $r > a$. The thermal contact resistance can be found by integrating the heat flux over the contact.[14]

If, for the problem depicted in Fig. 1, the radius and height of the cylinder are sufficiently large compared to the radius of the spot, the solution should mimic the analytic result for the half-space. Exploiting the symmetry, we use a one-quarter section (Figs. 3a and 3b) in the calculation. Note that there are no elements on either the $x=0$ and $y=0$ planes, or the insulated portion of the $z=0$ plane. The edge of the contact requires a highly refined mesh (Fig. 3c) because of the discontinuous flux along this curve. However, this level of refinement does not propagate into the remainder of the model because there are no other surfaces adjacent to the contact region. Away from the contact, the functions are not changing dramatically, and the discretization can be fairly crude. The ability to isolate the contact, therefore, greatly reduces the number of nodes and elements in the model, thereby reducing the cost of the computation. An additional benefit is that construction of the grid requires much less time.

*Grid Generation*

A discretization that concentrates the nodes near the edge of the circular spot was produced using the PIGS[15] code. A preliminary discretization was first constructed in two regions. An outer annulus next to the edge was decomposed into two rows of elements (three rows of nodes). These nodes were arranged in radial rows to facilitate the extrapolation procedure to be discussed next. The elements for the inner disk region were uniform in size and somewhat larger than those in the outer region. To refine the edge of the disk further, the element sizes were then adjusted in a coordinated manner. This adjustment was accomplished by mapping the uniform elements onto the surface of a sphere centered at the origin and then projecting the nodal locations down onto the $z=0$ plane. The resulting mesh has a smooth (decreasing) transition in element size from the center to the edge, except at the junction of the two regions just discussed.

*Extrapolation*

The singular behavior of the flux at the contact edge is almost certain to create difficulties for any general-purpose numerical method. In a direct application of the boundary-element method, this discontinuity manifests itself in the form of nonphysical oscillations in the computed flux near the edge of the contact. Instead of monotonically increasing radially from the center of the disk, the flux decreases at an interior node closest to the edge. In trying to respond to the singularity, the computed flux at the edge is quite large, and this apparently causes the depressed value at the adjacent interior node.

Although more sophisticated approximations (i.e., quadratic elements) are likely to improve the results, it is not clear that this would eliminate the problem. It is conjectured that the observed numerical oscillations stem from trying to solve for a nonexistent quantity, namely the flux on the circular arc, and not from an inadequate functional approximation. If this is the case, then using higher-order elements will not alter this state of affairs. Instead of pursuing this course of action (which nevertheless should be investigated), an alternative strategy has been devised.

Based on the idea that one should not try to compute the flux on the contact edge, Eq. (1) is not employed when $X_0$ is an edge node. These equations are replaced by those that determine the flux at the edge by extrapolating from interior nodes. The simplest possible procedure is to use two nodes and linearly extrapolate to the boundary curve: let $P_i = (x_i, y_i, z_i)$, $1 \le i \le 3$, denote the coordinates of the three points ($i=3$, the edge point) and $u_i$ the corresponding flux (see

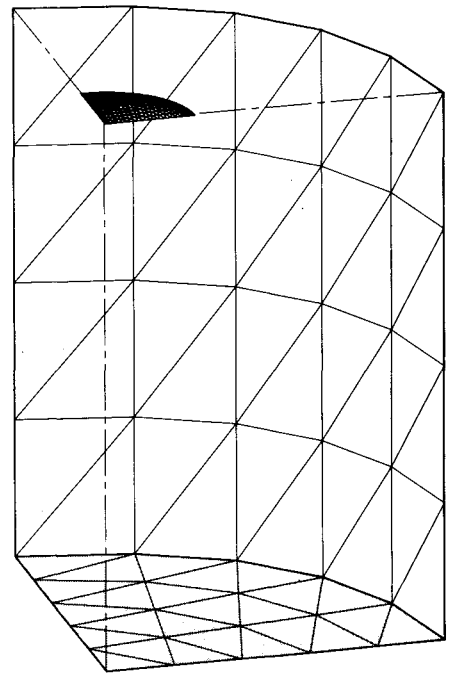

**Fig. 3a Circular contact discretization, whole model.**

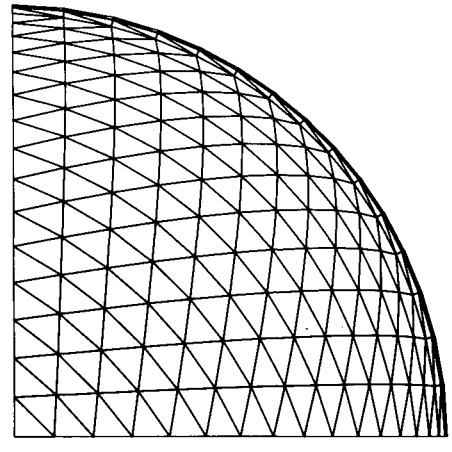

**Fig. 3b Circular contact discretization, contact only.**

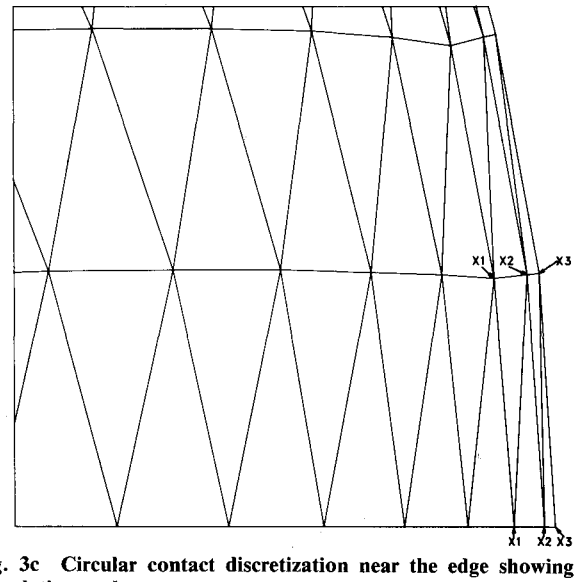


**Fig. 3c Circular contact discretization near the edge showing extrapolation nodes.**

Fig. 3c). The equation for $u_3$ is determined by stipulating that the distance between $\hat{P}_3 \equiv (P_3, u_3)$ and the line formed by $\hat{P}_1$ and $\hat{P}_2$ be a minimum. A little algebra yields

$$u_3 = (1 - t^*)u_1 + t^* u_2 \tag{7a}$$

where

$$t^* = -\frac{(P_1 - P_3)\cdot(P_2 - P_1)}{(P_2 - P_1)\cdot(P_2 - P_1)} \tag{7b}$$

*Results*

For the calculations, a contact radius of 0.8 was selected and two different outer cylinders were employed. The scale of the first cylinder, height equal to 5.0 and radius equal to 3.0, was chosen to correspond to problems considered by Mikic and Carnasciali.[7] (Figure 3 shows the discretization for this calculation.) As will be seen from the results, the second cylinder, with a height and radius of 15.0, more closely approximates the half-space geometry. The calculations were performed using a 12-point Gaussian quadrature algorithm for the numerical integrations required by Eq. (1). The contact and base temperatures were $T_0 = 100$ and $T_1 = 0$, respectively.

The radial heat flux distribution on the contact obtained using the two-point extrapolation is shown in Figs. 4a and 4b. In Fig. 4a, the boundary element results are compared with a finite-difference calculation[16] and an analytical approximation.[7] The computed results agree quite well, and the approximation method is clearly accurate. Figure 4b displays the results for both cylinders on an expanded vertical scale. The analytic curve for the larger cylinder is obtained from Eq. (6); the curve for the smaller cylinder is again the analytic approximation of Ref. 7 adjusted to same heat flow. The boundary element results agree with the analytical solution and are somewhat better than the finite difference method near the edge of the contact.

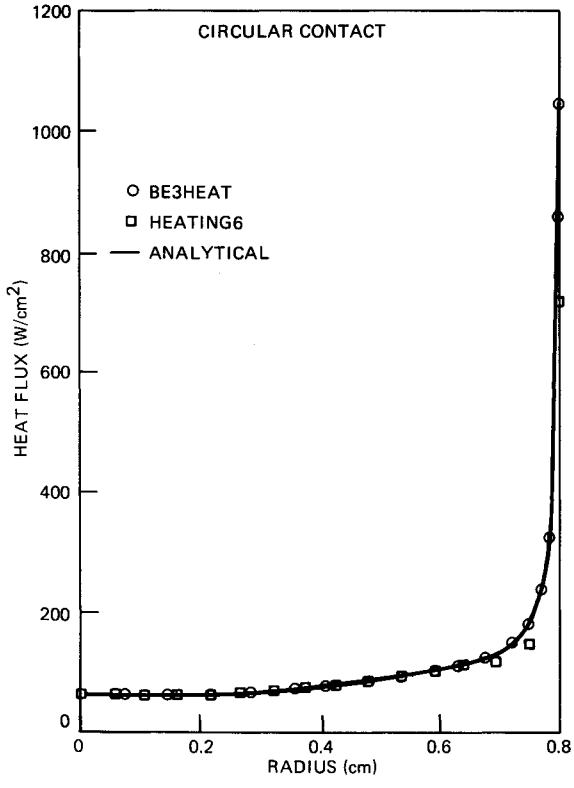


**Fig. 4a Circular contact heat flux distributions obtained from boundary-element code BE3HEAT and finite-difference code HEATING6.**

**Elliptical Contact**

When the contact region is modeled by an ellipse with a large eccentricity, the numerical problems at the tip of the major axis become even more acute. Currie[5] and Currie and Rogers[17] have investigated this problem quite extensively, using a variety of numerical schemes. Following Currie, an ellipse with an eccentricity of 0.998 has been chosen (semi-major axis = 0.154 cm, semi-minor axis = 0.009625 cm), and the cylinder of Fig. 1 has been replaced by a rectangular block, having a length and height of 2.54 cm and a width of 1.27 cm. Figure 5 displays the geometry and discretization for this problem. The side walls of this block (the planes $x = 2.54$ and $y = 1.27$) are insulated surfaces, whereas the bottom ($z = 2.54$) and contact surfaces are held at constant temperature ($T_1 = 0$ and $T_0 = 100$, respectively).

*Grid Generation*

To accommodate the strongly singular behavior at the tip, $(x,y) = (0.154, 0.0)$, a preliminary PIGS discretization was produced that had a gradual reduction in element size as the tip of the ellipse was approached. To refine this narrow region sufficiently, this discretization was then adjusted in a manner similar to that used for the circular contact. By mapping the original grid onto a surface (obtained by revolving a parabola around the $x$ axis) and then projecting the nodal coordinates back down to the contact, the degree of refinement achieved can be modified simply by changing the equation of the surface. This is easily accomplished by altering a few program statements; in this way, several different refinements can be tried without having to generate an entire new grid with the PIGS code. The mapping technique allows greater flexibility than is available in the PIGS code for smoothly adjusting element size.

The resultant discretization (Fig. 5) enables the extrapolation technique to be easily applied for most of the edge curve by extrapolating along constant $x$ (vertical) lines. (The major axis of the elliptical spot is along the $x$ axis of the coordinate system.) Near the tip of the ellipse, this technique is no longer possible, and therefore the extrapolation was performed along nearly constant $y$ lines.

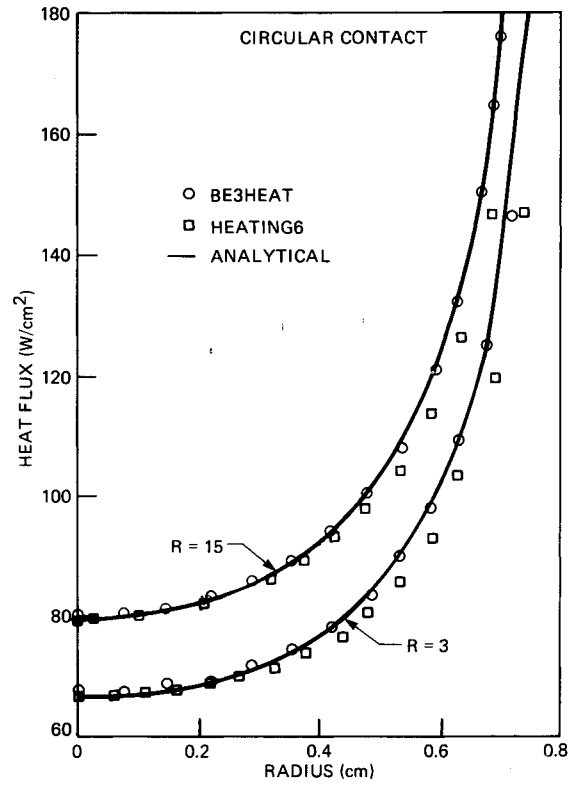


**Fig. 4b Heat flux distribution, expanded vertical scale.**

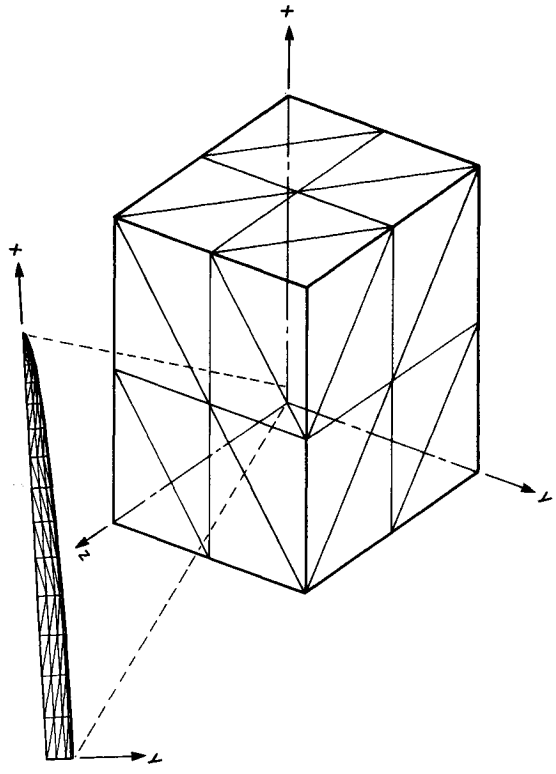


Fig. 5 Elliptical contact discretization.

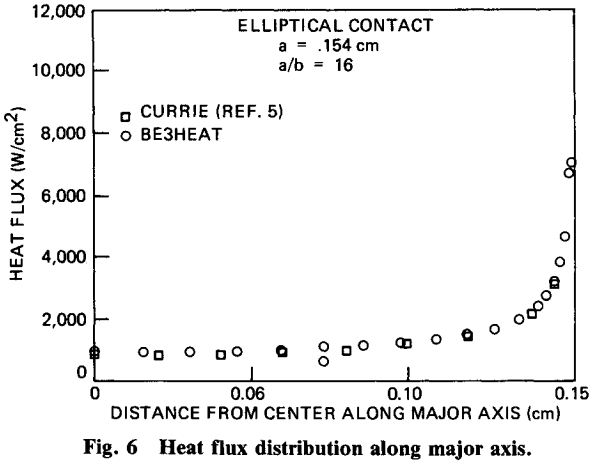


Fig. 6 Heat flux distribution along major axis.

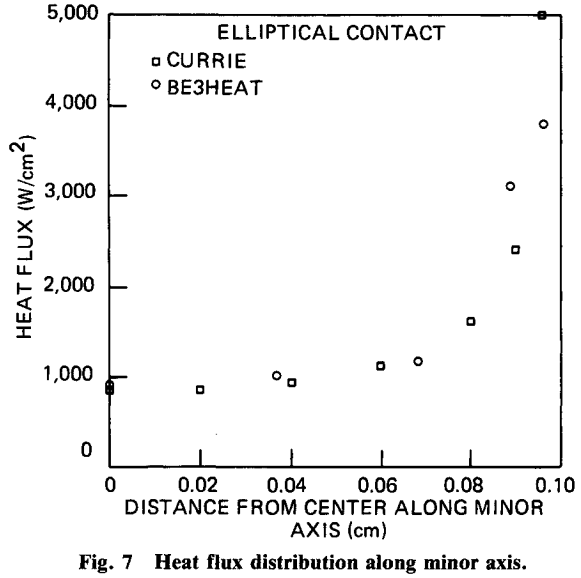


Fig. 7 Heat flux distribution along minor axis.

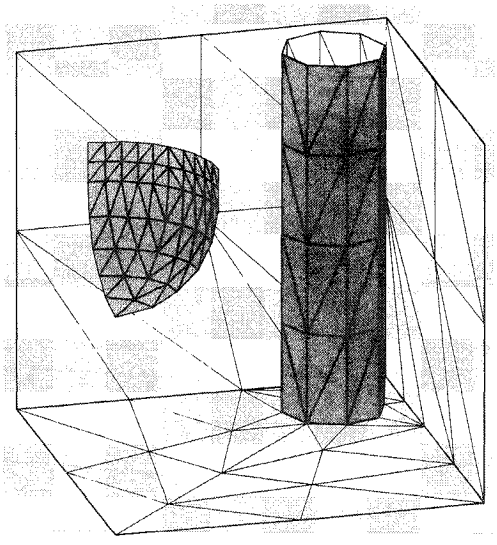

Fig. 8 Discretization of tank for heat-transfer analysis.

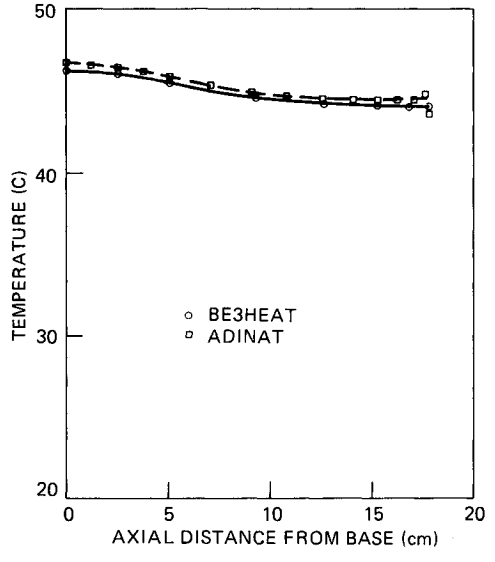


Fig. 9 Temperature distribution along edge of cathode.

Using the extrapolation technique, the computed heat flux on the contact was a smoothly increasing function out to the edge, even at the tip of the ellipse. The calculations also agreed reasonably well with the results reported by Currie[5]; a comparison of the heat flux values along the axes of the ellipse is shown in Figs. 6 and 7.

## Thermal Analysis of an Electroplating Cell

As mentioned in the introduction, a highly idealized model of the thermal processes in an electroplating tank will be considered. The tank, shown in Figs. 2 and 8, is an example of a reasonably complicated geometry that can be easily and efficiently handled using a specialized Green's function. The heat generated at the electrode surfaces was modeled by a constant heat flux, and it was assumed that the top (electrolyte/air interface) and the bottom of the tank behaved as insulating surfaces. The temperature of the side walls was maintained at the environmental temperature.

To simplify the future coupling of electroplating and heat-transfer calculations (i.e., setting the heat flux boundary conditions to be a function of the computed electrical current density), the discretization employed for the thermal analysis was essentially the same as that used for the electroplating simulations.[13] However, some modifications were required due to the different form of the boundary conditions imposed by the

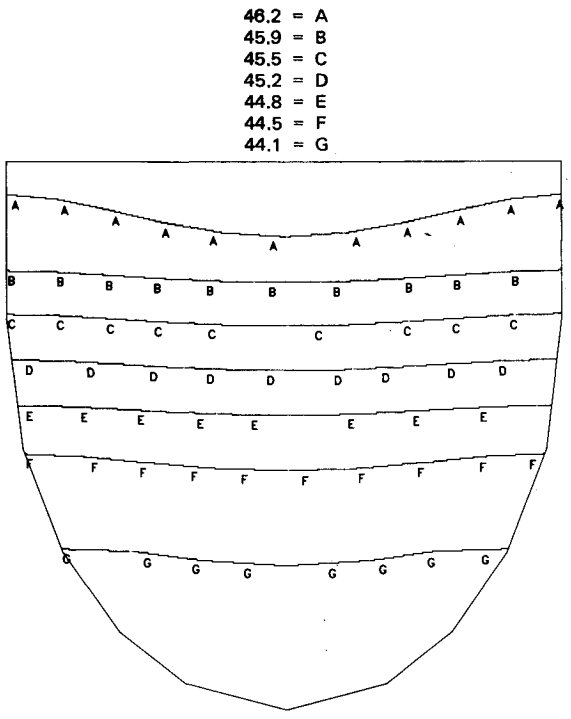


**Fig. 10 Isotherms on cathode surface, viewed along $X = Y$ plane.**

heat-transfer problem. For the electroplating simulations, the side walls and bottom of the tank were insulated; as there was no change in the boundary condition at the bottom edge of the tank, a coincident nodal structure at this junction was not required. In the thermal model, the boundary conditions switch from specified temperature to specified flux, requiring the use of double nodes[2] and, hence, a consistent discretization in moving from one plane to the other. With this exception, the nodes and elements in the two models correspond.

From the electroplating viewpoint, the primary quantity of interest in this problem is the temperature distribution on the cathode surface. As in the contact problem, use of the appropriate Green's function conveniently allows for a very fine mesh on the region of interest by isolating it from the other surfaces. The calculated temperature profile along the $y=0$ edge of the cathode is displayed in Fig. 9. Isotherms on the cathode are shown in Fig. 10. These results were corroborated by a finite-element calculation using ADINAT.

## Conclusions

Three-dimensional heat transfer problems posed in regions with symmetry can be effectively handled by the boundary-element method. By removing symmetry planes from the calculation, a specialized Green's function simplifies the task of constructing a discretized model and allows the nodes and elements to be concentrated on the region of interest. This technique permits an accurate solution without excessive computing cost. Although the contacts discussed here were simple symmetric shapes, the method clearly extends to planar or nonplanar contacts with arbitrary geometry. Of course, lacking the symmetry, the entire contact, not just a quarter section, must be used in the computation. Nevertheless, the insulated boundary adjacent to the contact can always be incorporated into the Green's function; thus, the contact can continue to be isolated from the rest of the model.

The difficulties caused by the singular behavior of the heat flux along the contact edge were solved by two-point linear extrapolating from the interior. Reasonable fluxes near the contact edge were obtained by this method, even for a highly elliptical geometry. This technique places constraints on the discretization, but these requirements should, in general, be easy to accommodate. Despite the simplicity of the approach, the extrapolation procedure performed quite well; higher-order extrapolation methods should prove even more effective and are currently being investigated.

## Acknowledgments

This research was sponsored by the Y-12 Development Division, Martin Marietta Energy Systems Inc., under contract DE-AC05-84OR21400 with the U.S. Department of Energy. The authors would like to thank Professor J.T. Rogers for his assistance and Professors J.V. Beck and J.S. Bullock for their helpful discussions.

## References

[1]Brebbia, C.A., Telles, J.C.F., and Wrobel, L.C., *Boundary Element Techniques,* Springer-Verlag, New York, 1984.

[2]Schneider, G.E. and LeDain, B.L., "Boundary Integral Equation Method and Corner Problem for Steady Heat Conduction," *Progress in Astronautics and Aeronautics: Heat Transfer, Thermal Control, and Heat Pipes,* Vol. 70, edited by W. Olstad, AIAA, New York, 1980, pp. 63–76.

[3]Schneider, G.E., "Thermal Resistance Due to Arbitrary Dirichlet Contacts on a Half-Space," *Progress in Astronautics and Aeronautics: Thermophysics and Thermal Control,* Vol. 65, edited by R. Viskanta, AIAA, New York, 1979, pp. 103–119.

[4]Braun-Angott, P., "A Boundary Integral Equation Method for the Temperature Analysis in Flat Rolling," *BETECH 86,* edited by J.J. Connor and C.A. Brebbia, Computational Mechanics Pub., Southampton, England, UK, 1986, pp. 237–248.

[5]Currie, T.C., "Heat Transfer Between Contacting Non-Conforming Surfaces: Experimental and Numerical Studies with Special Emphasis on Problems Involving Contact Patches of High Ellipticity," Ph.D. Thesis, Dept. of Mechanical and Aeronautical Engineering, Carleton Univ., Ottawa, Canada, 1984.

[6]Yovanovich, M.M., "General Expressions for Circular Constriction Resistances for Arbitrary Flux Distribution," *Progress in Astronautics and Aeronautics: Radiative Transfer and Thermal Control,* Vol. 49, edited by A.M. Smith, AIAA, New York, 1975, pp. 381–396.

[7]Mikic, B. and Carnasciali, G., "The Effect of Thermal Conductivity of Plating Material on Thermal Contact Resistance," *Journal of Heat Transfer,* Vol. 92, New York, Aug. 1970, pp. 475–482.

[8]Currie, T.C. and Rogers, J.T., "Heat Transfer Between Contacting Non-Conforming Surfaces with Application to CANDU Reactor Safety Analysis," *Proceedings of the ICHMT Seminar on Nuclear Reactor Safety Heat Transfer,* Hemisphere, New York, 1980.

[9]Yovanovich, M.M., "Thermal Constriction Resistance of Contacts on a Half-Space," *Progress in Astronautics and Aeronautics: Radiative Transfer and Thermal Control,* Vol. 49, edited by A.M. Smith, AIAA, New York, 1975, pp. 397–418.

[10]Keltner, N.R. and Beck, J.V., "Unsteady Surface Element Method," *Journal of Heat Transfer,* Vol. 103, Nov. 1981, pp. 759–764.

[11]Beck, J.V. and Keltner, N.R., "Transient Thermal Contact of Two Semi-Infinite Bodies Over a Circular Contact Area," *Progress in Astronautics and Aeronautics: Spacecraft Radiative Transfer and Temperature Control,* Vol. 83, edited by T.E. Horton, AIAA, New York, 1982, pp. 61–82.

[12]Gipson, G.S., Camp, C.V., and Radhakrishnan, N., "Phreatic Surface and Subsurface Flow with Boundary Elements Using an Advanced Green's Function," *BETECH 86,* edited by J.J. Connor and C.A. Brebbia, Computational Mechanics Pub., Southampton, England, UK, 1986, pp. 385–394.

[13]Gray, L.J., Giles, G.E., and Bullock, J.S., "Progress on Boundary Element Techniques for Electroplating Simulation," *BETECH 87,* edited by C.A. Brebbia and W.S. Venturini, Computational Mechanics Publications, Boston, MA, 1987, pp. 161–173.

[14]Carslaw, H.S. and Jaeger, J.C., *Conduction of Heat in Solids,* Oxford Univ. Press, London, 1959, pp. 214–216.

[15]*PIGS User's Manual,* PAFEC Ltd., Strelley Nottingham, U.K., 1986, pp. 214–216.

[16]Elrod, D.C., Giles, G.E., and Turner, W.D., "HEATING6: A Multidimensional Heat Conduction Analysis with the Finite Difference Formulation," Oak Ridge National Lab., Oak Ridge, TN, ORNL/NUREG/CSD-2/V2, Oct. 1981.

[17]Currie, T.C. and Rogers, J.T., "Heat Transfer Between Rough Surfaces in Contact over a Highly Elliptical Contour Area: Comparison of Experimental and Numerical Results," *Proceedings of the Eighth International Heat Transfer Conference,* Hemisphere Publishing, New York, 1986, pp. 639–644.